IEEE Access
Multidisciplinary | Rapid Review | Open Access Journal

Date of publication xxxx 00, 0000, date of current version xxxx 00, 0000.

Digital Object Identifier 10.1109/ACCESS.2017.Doi Number

Fabrication of Silicon Hierarchical Structures for Solar Cell Applications

Hsin-Ping Wang, * Periyanagounder Dharmaraj, An-Cheng Li, and Jr-Hau He*

Computer, Electrical and Mathematical Sciences and Engineering (CEMSE) Division, King Abdullah University of Science & Technology (KAUST), Thuwal 23955-6900, Kingdom of Saudi Arabia

Corresponding author: Jr-Hau He (jrhau.he@kaust.edu.sa), and Hsin-Pin Wang (hpwang0813@gmail.com).

"This work was financially supported by the King Abdullah University of Science and Technology (KAUST) Office of Sponsored Research (OSR-2016-CRG5-3005), KAUST Sensor Initiative, KAUST Solar Center, and KAUST baseline funding."

ABSTRACT Hierarchical silicon structures consisting of micropyramids and nanowire arrays are fabricated by two-step chemical etching processes aimed at achieving cost and time effectiveness constraints without using any expensive vacuum system or complicated lithography process. The hierarchical structures can suppress the average reflectance to as low as 4.3% from 300 to 1100 nm without causing poor minority carrier lifetimes, exhibiting excellent broadband light-harvesting abilities with minimal recombination losses, which is the key point to design high performance nanostructured solar cells. By utilizing hierarchical structures in practical solar cells application, the short-circuit current density (J_{SC}) shows a significant enhancement from 21.5 to 28.7 mA/cm^2, and the conversion efficiency is enhanced by a factor of 35%. Such a significant enhancement is attributed not only to the superior light harvesting achieved by hierarchical structures but also to the benefit of small electrical losses in the solar cells. Thus, the concept and technique presented in this study open avenues for developing high-performance structure solar devices.

INDEX TERMS: Hierarchical structures, Micropyramids, Light-harvesting, Power conversion efficiency, Surface recombination.

I. INTRODUCTION

Solar power has been esteemed to be an inexhaustible, renewable, and environmentally-friendly energy. In order to make a transition from non-renewable fossil fuels towards renewable solar energy sources, significant advances in energy conversion technologies are urgently needed. Many kinds of photovoltaics have been developed to efficiently convert solar energy into electricity such as crystalline Si solar cells, thin-film solar cells, III-V solar cells, dye-sensitized solar cells, and organic solar cells [1-4]. No matter what kinds of photovoltaics, the success of high-performance solar devices arguably rests on two factors: photon absorption and photocarrier extraction [5-9].

Surface texturing plays a critical role in enhancing the photon absorption in Si solar cells due to the high optical losses causing from light reflection from the high-refractive-index Si surface. The typical light-harvesting texture in Si photovoltaic market is micropyramidal structures [10]. However, there is still up to 20% reflection loss over the broadband wavelengths and angles of incident by using micropyramidal structures, which severely limits the photovoltaic performance [11]. Subwavelength structures have been considered as a promising alternative candidate to eliminate the reflection over broadband wavelength regions [12-15]. Their light-harvesting properties have been extensively studied by optimizing the morphologies of nanostructures [12,15,16]. In addition, since the feature sizes of nanostructures are in the same range as the diffusion length of minority photocarriers, structural designs such as a radial junction can minimize the carrier recombination due to short transport distances and then facilitate photocarrier collection, resulting in increased short-circuit current density (J_{SC}) and open-circuit voltage (V_{OC}) [17].

Such tremendous benefits offered by nanostructures should be directly expressed as a significant increase in photocurrent, and then the overall performance of solar devices. However, it is found that the nanostructure with better light-harvesting abilities does not always bring an enhancement of the solar energy conversion efficiency, but usually comes with more serious electrical losses in solar devices due to an enlarged surface area (*e.g.*, long nanowires (NWs)). Incorporation of high aspect-ratio nanostructures into solar cells leads to an excessive junction, high surface recombination, and unconformal

This article has been accepted for publication in a future issue of this journal, but has not been fully edited. Content may change prior to final publication. Citation information: DOI 10.1109/ACCESS.2018.2885169, IEEE Access

deposition of the antireflective (AR) layers, passivation layers, or metal electrodes over the surfaces of nanostructures. The gain in solar energy conversion efficiency *via* improved light harvesting is counterbalanced by poor electrical properties of solar devices, yielding an unsatisfactory performance of solar cells [18,19]. Consequently, there are challenges toward finding a balance between light harvesting and charge recombination.

Since the incorporation of nanostructures causes an unavoidable increase in surface area, designing the structures with superior light-harvesting properties with minimal recombination loss plays an important role to achieve high performance of nanostructured solar cells. The hierarchical architectures that combine materials of different classes, electrical/optical properties and scales provide synergistic and tailorable performance in light harvesting [20-22]. Note that they demonstrate superior AR abilities than that consist of purely high-aspect ratio nanostructures, realizing great light-harvesting properties with minimal surfaces (*i.e.*, surface recombination) [8]. Here, we proposed a controllable hierarchical structure consisting of micropyramids and NWs by mask-free chemical etching processes. Combining metal-assisted chemical etching with alkaline anisotropic chemical etching, large-area hierarchical structures can be obtained by cost- and time-effective manufacturing technology without using any expensive vacuum system or complicated lithography processes.

In this study, different morphologies of the Si hierarchical structures were demonstrated. To simultaneously probe both optical and electrical properties of hierarchical structures, experimental and simulated AR properties and minority carrier lifetimes of Si with different surfaces are thoroughly studied. The hierarchical structures with 1.5 μm NWs exhibit the average total reflectance (R_{total}) as low as 4.3% from 300 to 1100 nm (as compared to polished Si (38.5%) and micropyramidal structures (20.6%)). Moreover, the light-scattering behavior increases with the incorporation of NWs on micropyramids, contributing to an increase in light-matter interactions and effective optical thickness. The carrier lifetimes of hierarchical structures exhibit the similar values compared with those of micropyramidal structures and planar Si, indicating our hierarchical structures have the ability to increase photon absorption without compromising photocarrier extraction. To verify their optoelectrical properties into practice, Si homojunction solar cells are fabricated on cost-effective CZ *p*-type Si wafers with different surfaces. Compared to the solar cells with a planar surface, the J_{SC} increases from 21.58 to 28.70 mA/cm^2 by utilizing the Si hierarchical structures with only 0.5 μm NWs, exhibiting the excellent light trapping and sufficient carrier collection efficiency. The solar cell with optimized hierarchical structure exhibits the efficiency of 10.47% without any passivation or AR layers. Such hierarchical structures achieve effective light harvesting and carrier collection, offering an attractive solution for next-generation solar devices.

II. EXPERIMENTAL SECTION

In this work, the fabrication of solar cells follows standard procedures. Single crystalline p-type Si (001) wafers with ρ=5-10 Ω-cm were cleaned in acetone, followed by an HF dip to remove the native oxide from the surfaces. The cleaned substrates were etched by a potassium hydroxide solution (KOH: IPA: H2O = 1:1:17) at 85°C for 20 min for micropyramid-textured etching. Subsequently, the textured substrates were immersed into an aqueous HF and $AgNO_3$ mixture solution and treated at room temperature. The concentrations of HF and $AgNO_3$ were 4.6 M and 30 mM, respectively. Various length of Si NWAs on the micropyramid-textured substrates was obtained by different etching times varying from 5 to 30 min. For device fabrication, the source of phosphorus doping using P_2O_5 solution at p-type substrate was formed as an n-emitter layer. The P_2O_5 solution was spin-coated on the samples and then annealed at 950°C for 20 min at atmosphere. After removal of the surface thermal oxides generated from the annealing process by HF, the front grid electrode (Ti/Ag) and the back electrode (Al) were deposited by e-gun evaporation. Other solar cells with different surfaces of polished and micropyramid-textured were fabricated under the identical condition for comparison. Morphological studies of the micropyramid-textured and hierarchical structures with NWAs were performed with JEOL JSM-6500 field emission SEM. The reflectance measurements were carried out by a standard UV-vis spectrometer (JASCO ARN-733) with an integrating sphere. The reflected light was collected by the integrating sphere during the measurement of R_{total}. For the specular reflection spectra, the coherent reflection of a collimated incident light beam was determined by collecting the specularly reflected cone of light within an acceptance angle of 5º.

The photovoltaic J–V characteristics measurement was carried out with a Keithley 2400 source meter under the illumination of AM 1.5G solar simulator (100 mW/cm^2). The effective lifetime after chemical passivation by an iodine ethanol (I/E) solution of wafers was investigated by QSSPC method. The external quantum efficiency (EQE) was measured by coupling the Halogen lamp to a monochromator. The theoretical calculations based on FDTD were employed for the simulation of the $|E_z|$ distribution of the different Si structures. The Raman spectroscopy was obtained by a micro-Raman Jobin Yvon T64000 system equipped with a coherent VerdiV10 532 nm laser as the excitation source, and the signals were detected with the back illuminated UV enhanced CCD detector.

This article has been accepted for publication in a future issue of this journal, but has not been fully edited. Content may change prior to final publication. Citation information: DOI 10.1109/ACCESS.2018.2885169, IEEE Access

III. RESULTS AND DISCUSSION

Fig. 1a-1c illustrate the flowchart of the process schematic of the Si hierarchical structure fabrication. First, the Si micropyramids were fabricated on *p*-type monocrystalline (100) Si substrates *via* an anisotropic etching process using a solution of KOH and IPA at 85 °C. After 20 min treatment, micropyramids were formed with a width of 5-8 μm on the surfaces of Si substrates. Subsequently, hierarchical NWs were constructed from the surface of the micropyramids by means of a silver-assisted chemical etching process in a solution of HF and $AgNO_3$ at room temperature followed by the removal of Ag by HNO_3. Fig. 1d-1g are scanning electron microscopy (SEM) images of the Si hierarchical structures with different silver-assisted chemical etching durations of 5, 10, 20, and 30 min, respectively. The morphologies of hierarchical structures are determined by the duration of silver-assisted chemical etching. Briefly, in the first 5 min, the surface of micropyramids becomes rough and porous. With the longer etching time, the etched pits form NW arrays (NWAs), and the lengths of NWs from 0.5 to 1.5 μm correspond to the etching time of 10, 20, and 30 min. The linear dependence of the length of NWs and etching time indicates the etching rate is constant [23]. The NWAs are vertical on the facet of the micropyramids, revealing that the silver-assisted electroless chemical etching process is performed by selectively etching along the direction perpendicular to each face of the tetrahedron [24]. By using the two-step chemical etching, the hierarchical structures uniformly distributed on the entire wafer surface, demonstrating the feasibility of wafer-scale processing in solar cell applications.

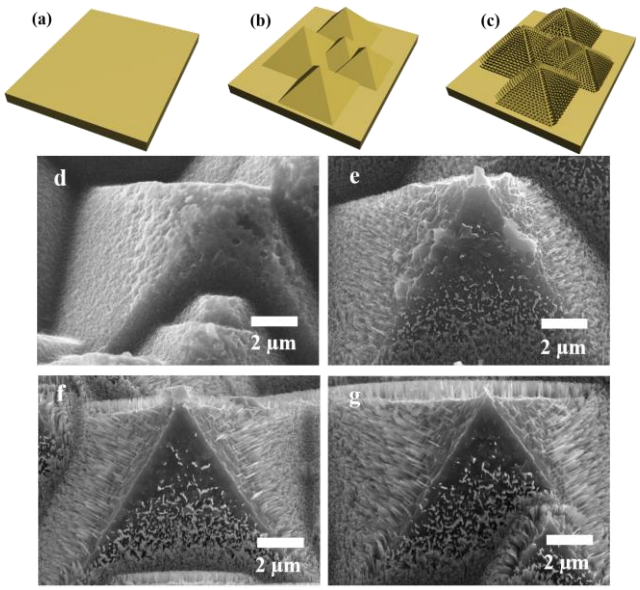

Fig. 1: (a)-(c) illustrate the flowchart of the experimental process for fabricating Si hierarchical NWAs/micropyramid structure. The 45°-tilted SEM images of Si NWAs/micropyramid structures with various lengths of Si NWAs which fabricated with the etching time of (d) 5 min, (e) 10 min, (f) 20 min, and (g) 30 min.

To investigate the light-harvesting ability of hierarchical structures, the wavelength-dependent total reflectance (R_{total}), specular reflectance (R_{spec}), diffuse reflectance (R_{diff}), and haze ratio of different Si surfaces: planar surfaces, micropyramidal surfaces, and hierarchical surfaces with different lengths of NWs were measured over a spectrum ranging from 300 to 1100 nm (Fig. 2 and Fig. S1 in the Supporting Information). The R_{total} of the surface with hierarchical structures shows a significant reduction as compared with that of the planar and micropyramidal surface over broadband ranges. Once the hierarchical structures are introduced, the average R_{total} reduced from 38.5% to 8.2%, 7.6% and 4.3% for the hierarchical structures with 0.5, 1.0, and 1.5 μm NWs, which is also much lower than that of the traditional micropyramidal surface (20.6%), exhibiting the superior AR abilities of hierarchical structures. The light-harvesting ability of hierarchical structures was also investigated by Raman measurement (Fig. S2 in Supporting Information).

The significant elimination in reflectance for the hierarchical structures can be explained by several effects. First, the subwavelength features of the NWAs on the micropyramidal surfaces behave like an effective medium with an effective refractive index (n_{eff}) gradually decreasing from Si substrates to the air. Incident light strikes on the subwavelength structures as if it comes across a thin AR layer with an intermediate n_{eff} between refractive index indices of air and Si, increasing the amount of light entering the structures. Hierarchical structures with long NWs provide a smoother n_{eff} transition from air to Si micropyramids compared with that with short NWs, aiding more incident photon entering to the substrates, which lowers reflectance losses and therefore enhances absorptance [7,12,25]. Second, when incident light encounters the micropyramids, these microscaled structures lead to effective multiple scattering, increasing the probability of light absorption and prolonging the optical path in the solar devices. The scattering behavior can be determined by haze ratio (Fig. 2b). Since light rays scatter in many different directions, optical scattering can be separated into the specular part and diffuse part. The haze ratio is defined as the ratio of diffuse reflection to total reflection to evaluate the light scattering properties of textured surfaces [26]. It is noted that the after NWs formed on micropyramids, the light scattering behavior of the micropyramidal surface can be further enhanced (*i.e.*, increased haze ratio in Fig. 2b), which is beneficial to light absorption within solar devices. Since the haze ratio is exponentially increased with the roughness, the enhanced light scattering might be attributed to an increased surface roughness for hierarchical structures [27,28].

This article has been accepted for publication in a future issue of this journal, but has not been fully edited. Content may change prior to final publication. Citation information: DOI 10.1109/ACCESS.2018.2885169, IEEE Access

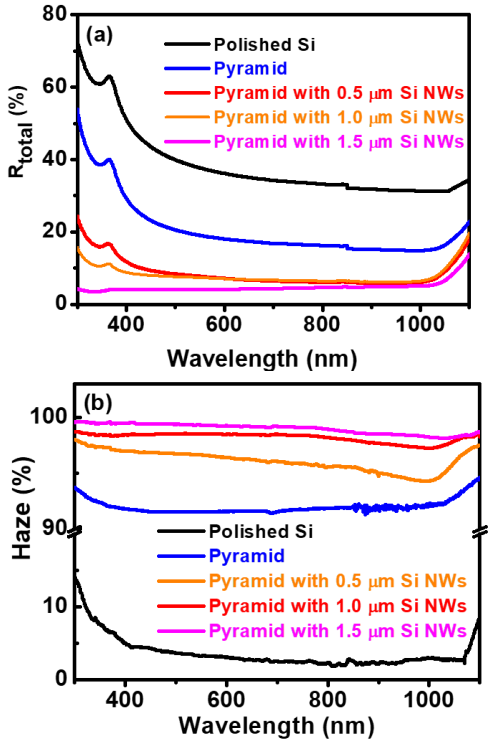

Fig. 2: (a) Total reflectance and (b) haze ratio of planar Si, micropyramid-textured Si, and Si NWAs/micropyramid binary structure with various lengths of Si NWAs.

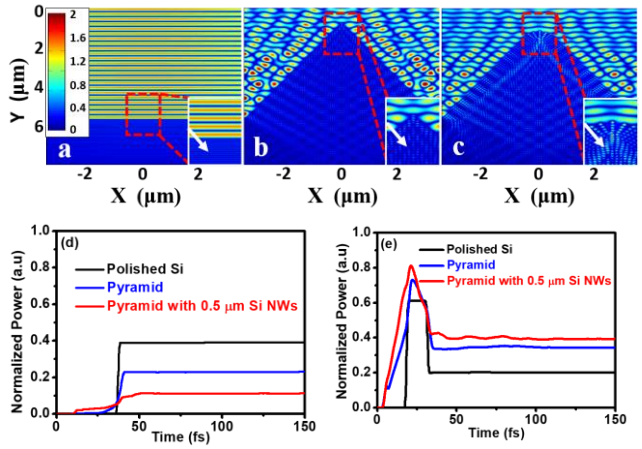

Fig. 3: Time-averaged and normalized TE electric field distribution, |Ez|, simulated by FDTD analysis. (a)-(c) is simulated with the incident wavelength of 500 nm on the structures: (a) the polished surface, (b) the micropyramid-textured surface, and (c) the 0.5 μm Si NWAs on micropyramid-textured surface. (d) and (e) present the normalized optical power: (d) detected at 0.5 μm above excitation source, and (e) detected at 1 μm below the surface of Si, as a function of time. The insets in (a)-(c) are the enlarged images at the top Si surface.

To gain insight into the light propagation across different surfaces, we simulated light propagation with the selected wavelength of 500 nm using FDTD analysis. Fig. 3a-3c show the time-averaged TE-polarized electric field intensity ($|E_z|$) distributions of a planar surface, a micropyramidal surface, and a surface with hierarchical structures with 0.5 μm NWAs, and the insets show the high magnification images in the interface region of air and Si to highlight the light-trapping effect. The absorption behavior can be described in terms of the field distribution inside NWAs and micropyramids. As compared with the results of Si with planar and micropyramidal surfaces, the field intensities of hierarchical structures have a great enhancement within the NWs and the micropyramids (as shown using arrow mark). To further investigate the AR ability and the absorption over the *p-n* junction, where the photocarriers can be efficiently separated, the optical powers detected at 0.5 μm above the excitation source (*i.e.*, reflection) and at 1 μm below the surfaces (*i.e.*, absorption) were performed in Fig. 3d and 3e. The steady-state power values of reflection for the three structures are 0.39 (polish), 0.21 (micropyramids), and 0.10 (hierarchical structures), which agree with the experimental results of reflection measurement at 500 nm (Fig. 2a). The steady-state absorption values for the three structures are 0.20 (polish), 0.34 (micropyramids), and 0.39 (hierarchical structures), demonstrating the number of the photons reaching the active region can be dramatically increased by introducing hierarchical structures.

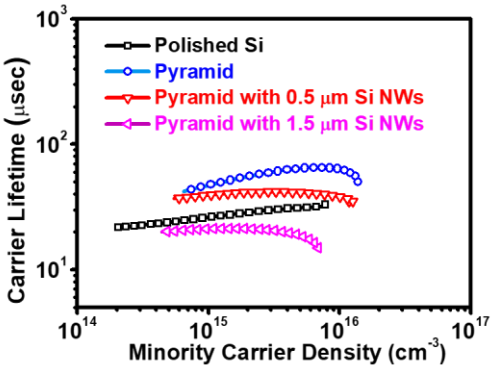

Fig. 4: Effective minority carrier lifetime of Si wafers with different surfaces

In order to take the optical absorption and electrical carrier recombination into account simultaneously, the minority carrier lifetime measuring by the quasi-steady-state photoconductance (QSSPC) technique is employed to evaluate the surface recombination after introducing those light-harvesting structures (Fig. 4). The lower minority carrier lifetimes of planar Si as compared with Si with micropyramidal surfaces might be attributed to the different ratio of (100) and (111) planes. The (100) plane exhibits two dangling bonds while the (111) plane has one, suggesting that the surface state density of (111) plane is lower than that of the (100) plane [29-32]. Pyramidal structures with a lot of (111) planes exposed due to the anisotropic etching nature exhibit the highest minority carrier lifetime. After NWs forming on the pyramidal surface, the minority carrier lifetime starts to decrease due to the increased surface area, increasing the surface recombination. To further increase the length of NWs, the carrier lifetime drops more and is below the value of planar

This article has been accepted for publication in a future issue of this journal, but has not been fully edited. Content may change prior to final publication. Citation information: DOI 10.1109/ACCESS.2018.2885169, IEEE Access

Si. Therefore, the most important thing in designing high efficiency textured solar devices is to find the balance between the optical gains and electrical losses caused by those light-harvesting structures. We then verified how the different structures influence the optoelectronic characteristics of solar devices. The *J-V* characteristics of solar cells with different structures were measured under the illumination of AM 1.5G solar simulator at room temperature as shown in Fig. 5a and 5b. It's clear to see a significant enhancement of J_{SC} from 21.5 (planar surface) to 28.7 mA/cm^2 (hierarchical structure with only 0.5 μm NWs) without any passivation and AR coatings. The enhancement of absorption caused from the great light harvesting of hierarchical structures contributes to the enhancement of the photocurrent, then resulting in a 35% enhancement in the efficiency of solar cells (from 7.75% to 10.47%).

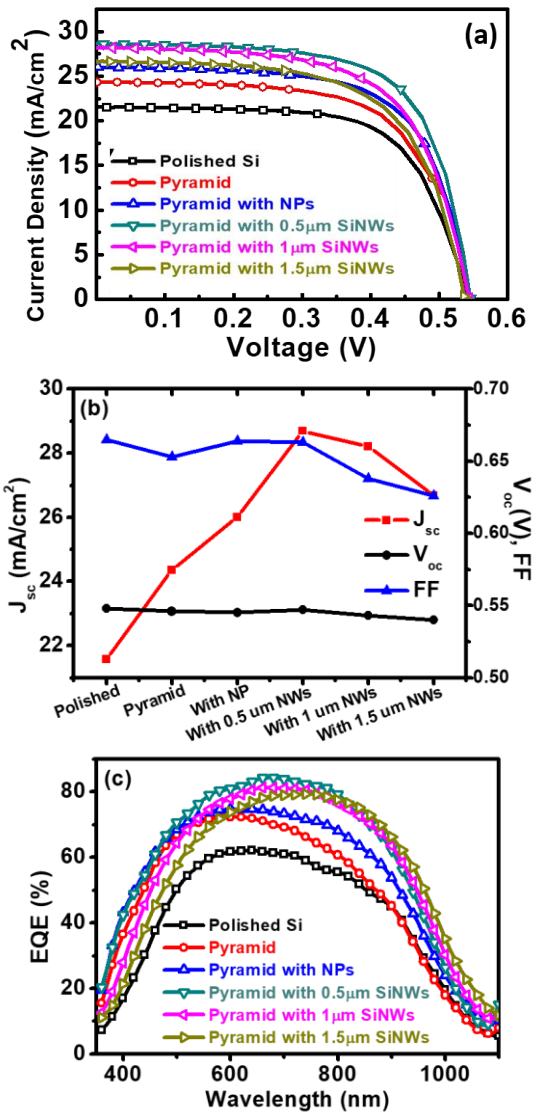

Fig. 5: (a & b) J-V characteristics of the solar cell with different morphological features and (c) EQE of different solar cell devices.

Although the hierarchical structures with longer NWs exhibit better AR abilities, the J_{SC} shows an opposite trend to their AR abilities, indicating the improved optical performance is counterbalanced by the expense of electrical properties for high aspect-ratio structures. The poor carrier collection of structures with long NWs counteracts the gain of J_{SC} coming from increased light absorption. Moreover, the decreases in J_{SC} and fill factor with increased length of NWs can also be ascribed to nonconformal deposition of the metal electrodes over a relatively high aspect ratio of the long NWAs.

In addition, the V_{oc} of the cells with different hierarchical architexure shows almost invariant with no significant decrease as compared with planar device, indicating that no serious V_{oc} loss is observed owing to the ameliorating effect of concurrently improved electrical and optical characteristics; making it possible to achieve high-performance solar cell devices. Therefore, the optimized structure for solar cells is the hierarchical structure with short NWs, which presents excellent light-harvesting abilities with minimal recombination losses.

In order to gain an insight into the J_{SC} improvement with wavelengths, the EQE spectra are measured from 350 to 1100 nm, as shown in Fig. 5c. As compared to the polished and micropyramid-textured Si, the hierarchical structured solar cell exhibits significant EQE enhancement in the broadband region of wavelengths. The EQEs of hierarchical structures decrease with the increasing length of the NWs, especially in the short-wavelength regions. Owing to the shallow corresponding absorption depths in short-wavelength regions, which is in the vicinity of the surface defects created by the metal-assisted chemical etching, the degeneration of EQE is more obvious [33]. The high recombination rate associated with samples with longer NWAs deteriorates the efficiency accordingly [34].

IV. CONCLUSION

In summary, the wafer-scale Si hierarchical structures are fabricated by cost- and time-effective two-step chemical etching processes. A significant improvement in light harvesting is investigated by experiments and simulations. The experimental average R_{total} can be as low as 4.7% over a broad spectrum from 300 to 1100 nm; the simulated absorption values within *p-n* junction can increase to almost 2 times higher than the planar surface by introducing hierarchical structures. The superior light-harvesting performance of the Si hierarchical structures is attributed to the gradient refractive index effect of NWs combined with the light scattering effect of micropyramids. Their excellent light harvesting contributes to a significant enhancement in J_{SC} from 21.5 to 28.7 mA/cm^2, and the conversion efficiency is enhanced by a factor of 35%. Such a significant enhancement is attributed to not only the superior light harvesting by hierarchical structures but also negligible electrical losses in solar cells. The achievement of hierarchical structured solar cells demonstrated here

makes the hierarchy concept highly attractive for scalable and high-performance solar cells.

References:

[1] J Zhao, A Wang, M. A. Green, F. Ferrazza, "19.8% efficient "honeycomb" textured multicrystalline and 24.4% monocrystalline silicon solar cells," *Applied Physics Letters*, vol. 73, pp. 1991-1993, Jul. 1998.

[2] B. O'Regan, M. Gratzel, "A low-cost, high-efficiency solar cell based on dye-sensitized colloidal TiO2 films," *Nature*, vol. 353, pp. 737-740, Oct. 1991.

[3] A. Shah, P. Torres, R. Tscharner, N. Wyrsch, H. Keppner, "Photovoltaic Technology: The Case for Thin-Film Solar Cells," *Science*, vol. 285, pp. 692, Jul.1999.

[4] H. Hoppe, N. S. Sariciftci, "Organic solar cells: An overview," *Journal of Materials Research*, vol. 19, pp. 1924-1945, March 2004.

[5] M. D. Kelzenberg, S. W. Boettcher, J.A. Petykiewicz, D. B. Turner-Evanas, MC. Putnam, EL. Warreb, JM Spurgeon, RM. Briggs, NS. Lewis, HA.Atwater, "Enhanced absorption and carrier collection in Si wire arrays for photovoltaic applications," *Nature Materials*, vol. 9, pp. 239-244, Feb. 2010.

[6] M. Law, L. E. Greene, J. C. Johnson, R. Saykally, & P. Yang, "Nanowire dye-sensitized solar cells,". *Nature Materials*, vol. 4, pp. 455-459, May 2005.

[7] J. Nelson, "Organic photovoltaic films," *Current Opinion in Solid State and Materials Science*, vol. 6,pp. 87-95, Jun. 2002.

[8] H.-P. Wang, T.-Y. Lin, C.-W. Hsu, M.-L. Tsai, C.-H. Huang, W.-R. Wei,M.-Y. Huang, Y.-J. Chien, P.-C. Yang, C.-W. Liu, L.-J. Chou, J.-H. He, "Realizing High-Efficiency Omnidirectional n-Type Si Solar Cells via the Hierarchical Architecture Concept with Radial Junctions," *ACS Nano*, vol. **7**, 9325-9335, Sept. 2013.

[9] M.-L. Tsai, W.-R. Wei, L. Tang, H.-C. Chang, S.-H. Tai, P.-K. Yang, S. P. Lau, L.-J. Chen, and J.-H. He, "Si Hybrid Solar Cells with 13% Efficiency via Concurrent Improvement in Optical and Electrical Properties by Employing Graphene Quantum Dots," *ACS Nano*, vol. 10, pp. 815-821, Dec. 2015.

[10] P. Campbell, M. A. Green, "Light trapping properties of pyramidally textured surfaces," *Journal of Applied Physics*, vol. 62, pp.243-249, Feb.1987.

[11] P. K. Singh, R. Kumar, M. Lal, S. N. Singh, B. K. Das, "Effectiveness of anisotropic etching of silicon in aqueous alkaline solutions," *Solar Energy Materials and Solar Cells*, vol. 70, pp. 103-113, Aug 2001.

[12] H.-C. Chang, K-Y. Lai, Y.-A. Dai, H.-H. Wang, C.-A. Lin, J.-H. He, "Nanowire arrays with controlled structure profiles for maximizing optical collection efficiency," *Energy & Environmental Science*, vol. 4, pp. 2863-2869, Feb. 2011.

[13] Y.-C. Chao, C.-Y. Chen, C.-A. Lin, Y.-A. Dai, & J.-H. He, "Antireflection effect of ZnO nanorod arrays," *Journal of Materials Chemistry*, vol. 20, pp. 8134-8138, Aug. 2010.

[14] H.-P. Wang, K.-T. Tsai, K.-Y. Lai, T.-C. Wei, Y.-L. Wang, J.-H. He, "Periodic Si nanopillar arrays by anodic aluminum oxide template and catalytic etching for broadband and omnidirectional light harvesting," *Opt. Express*, vol. 20, pp. A94-A103, Jan. 2012.

[15] H.-P. Wang, K.-Y. Lai, Y.-R. Lin, C.-A. Lin, J.-H. He, "Periodic Si Nanopillar Arrays Fabricated by Colloidal Lithography and Catalytic Etching for Broadband and Omnidirectional Elimination of Fresnel Reflection," *Langmuir*, vol. 26, pp. 12855-12858, Jul. 2010.

[16] J. Zhu, Z. Yu, G. F. Burkhard, C.-M. Hsu, S.T.Connor, Y.Xu, Q. Wang, M. McGehee, S. Fan, Y. Cui, "Optical Absorption Enhancement in Amorphous Silicon Nanowire and Nanocone Arrays," *Nano Letters*, vol**.** 9, pp. 279-282, Dec. 2008.

[17] E. C. Garnett, M. L. Brongersma, Y. Cui, M. D. McGehee, "Nanowire Solar Cells," *Annual Review of Materials Research*, vol. 41, pp. 269-295, Mar. 2011.

[18] H. Li, R. Jia, C. Chen, Z. Xing, W. Ding, Y. Meng, D. Wu, X. Liu, T. Ye, "Influence of nanowires length on performance of crystalline silicon solar cell," *Applied Physics Letters*, vol. 98, pp. 151116 (1-3), Apr. 2011.

[19] H.-P. Wang, D.-H. Lien, M.-L. Tsai, C.-A. Lin, H.-C. Chang, K.-Y. Lai, J.-H. He, "Photon management in nanostructured solar cells," *Journal of Materials Chemistry C*, vol. 2, pp.3144-3171, Feb. 2014.

[20] H. F. Zarick, W. R. Erwin, A. Boulesbaa, O. K. Hurd, J.A. Webb, A.A. Puretzky, D.B. Geohegan, R. Bardhan, "Improving Light Harvesting in Dye-Sensitized Solar Cells Using Hybrid Bimetallic Nanostructures," *ACS Photonics*, vol. 3, pp. 385-394, Jan. 2016.

[21] I. E. Khodasevych, L. Wang, A. Mitchell, G. Rosengarten, "Micro- and Nanostructured Surfaces for Selective Solar Absorption," *Advanced Optical Materials*, vol. 3, 852-881,

May 2015.

[22] C.-A. Lin, K.-Y. Lai, W.-C. Lien, J.-H. He, "An efficient broadband and omnidirectional light-harvesting scheme employing a hierarchical structure based on a ZnO nanorod/Si3N4-coated Si microgroove on 5-inch single crystalline Si solar cells," *Nanoscale*, vol. 4, pp. 6520-6526, Oct. 2012.

[23] S. L. Cheng, C. H. Chung, & H. C. Lee, "A Study of the Synthesis, Characterization, and Kinetics of Vertical Silicon Nanowire Arrays on (001)Si Substrates," *Journal of The Electrochemical Society*, vol. 155, D711-D714 Sep. 2008.

[24] X. Li, B. Tay, P. Miele, A. Brioude, & D. Cornu, "Fabrication of silicon pyramid/nanowire binary structure with superhydrophobicity," *Applied Surface Science*, vol. 255, pp. 7147-7152, May 2009.

[25] D. H. Raguin, & G. M. Morris, "Analysis of antireflection-structured surfaces with continuous one-dimensional surface profiles," *Applied Optics*, vol. 32, pp. 2582-2598, 1993.

[26] O. Kluth, *B. Rech, L. Houben, S. Wieder, G. Schope, C. Beneking, H. Wagner, A. Loffl, H.W. Schock, "*Texture etched ZnO:Al coated glass substrates for silicon based thin film solar cells," *Thin Solid Films*, vol. 351, pp. 247-253, Aug. 1999.

[27] C. K. Carniglia, "Scalar Scattering Theory For Multilayer Optical Coatings," *Optical Engineering*, vol. 18, pp. 104-115, Apr. 1979.

[28] C. C. Lin, W. L. Liu, C. Y. Hsieh, "Scalar scattering model of highly textured transparent conducting oxide," *Journal of Applied Physics*, vol. 109, pp. 014508 (1-9), Jan 2011.

[29] H.-P. Wang, T.-Y. Lin, M.-L. Tsai, W.-C. Tu, M.-Y. Huang, C.-W. Liu, Y.-L. Cheuh, J.-H. He, "Toward efficient and omnidirectional n-type Si solar cells: Concurrent improvement in optical and electrical characteristics by employing microscale hirerachical nanostructures," *ACS Nano*, vol.8, pp 2959-2969, Feb 2014.

[30] M. Edwards, S. Bowden, U. Das, "Effect of texuring and surface preparationon lifetime and cell performance in heterojunction solar cells," *Sol. Energy Mater.Sol.Cells*, Vol.92, pp 1373-1377, May 2008.

[31] U. Neuwald, H.E. Hessel, A. Feltz, U. Memmert, R.J. Behm, "Wet Chemical Etching of Si(100) Surfaces in Concentrated NH4F Solution: Formatin of (2×1)H Reconstructed Si(100) Terraces versus (111) Faceting," *Surface Science*, Vol. 296, pp.L8-L14, Oct 1993.

[32] H. Angermann, W. Henrion, A. Roseler, M. Reibin, "Wet Chemical Passivation of Si (111)- and Si (100)- Substrates," *Materials Science Engineering B*,Vol.73, pp.178-183, March 2000.

[33] L. H. Lin, X.Z. Sun, R.Tao, Z.C. Li, J.Y. Feng, Z. J. Zhang, "Photoluminescence origins of the porous silicon nanowire arrays," *Journal of Applied Physics*, vol**.** 110, pp. 073109 (1-7), Oct. 2011.

[34] T.-C. Yang, T.-Y. Huang, H.-C. Lee, T.-J. Lin, T.-J. Yen, "Applying Silicon Nanoholes with Excellent Antireflection for Enhancing Photovoltaic Performance," *Journal of The Electrochemical Society*, vol. 159, pp B104-B108, Dec. 2011.